FTIR Spectroscopic Characterization of the Cytochrome aa_3 from *Acidianus ambivalens*: Evidence for the Involvement of Acidic Residues in Redox Coupled Proton Translocation†

Petra Hellwig,*,‡ Cláudio M. Gomes,§,# and Miguel Teixeira#

Institut für Biophysik, Universität Frankfurt, Theodor-Stern-Kai 7 Haus 75, 60590 Frankfurt, Germany, Departamento de Química, Faculdade de Ciências e Tecnologia, Universidade Nova de Lisboa, 2825-114 Caparica, Portugal, and Instituto de Tecnologia Química e Biológica, Universidade Nova de Lisboa, Oeiras, Portugal

Received August 15, 2002; Revised Manuscript Received March 31, 2003

ABSTRACT: The aa_3-type quinol oxidase from *Acidianus ambivalens* is a divergent member of the heme-copper oxidases superfamily, namely, concerning the putative channels for intraprotein proton conduction. In this study, we used electrochemically induced FTIR difference spectroscopy to identify residues involved in redox-coupled protonation changes. In the spectral region characteristic for the ν(C=O) mode from protonated aspartic or glutamic acid side chains, a number of prominent features can be observed between 1790 and 1710 cm^{-1}, clearly indicating the reorganization or protonation of more than four protonatable residues upon electron transfer. A direct comparison of the Fourier-transform infrared difference spectra at different pH values reveals the noteworthy high pK of >8 for some of these residues, and the protonation of two of them. These acidic residues may play a role in the proton transport to the oxygen reducing site, in proton pumping pathways, or in protonation reactions concomitant with quinone reduction. Whereas the residues contributing between 1790 and 1750 cm^{-1} have the typical position of an aspartic/glutamic acid side chain buried in the protein, a position closer to the surface is suggested for the residues contributing below approximately 1730 cm^{-1}. The possible involvement of residues contributing between 1750 and 1720 cm^{-1} in the quinone binding site is demonstrated on the basis of experiments in the presence and absence of ubiquinone-2 and of the native electron carrier of the *A. ambivalens* respiratory chain, caldariella quinone. Most signals seen here are not observable in comparable spectra of typical members of the heme copper oxidase superfamily and thus reflect unique features of the enzyme from the hyperthermo-acidophilic archaeon *A. ambivalens*.

Heme copper terminal oxidases are the last enzymes of aerobic respiratory chains, catalyzing the stepwise reduction of oxygen to water. In the course of this process, electron and proton transfer are efficiently coupled to contribute to the formation of an electrochemical gradient, which drives ATP synthesis. The field of respiratory oxidases can greatly profit from the study of enzymes originating from phylogenetically distant microorganisms, which together with the accumulating genomic data, significantly contribute to a wider view of the functional, structural, and mechanistic diversity found among prokaryotic terminal oxidases (for recent reviews see refs *1*−*5*).

In the last years, functional and mechanistic studies on the aa_3 quinol oxidase isolated from the thermoacidophilic archaeon *Acidianus* (*A.*) *ambivalens* (T_{opt} = 80 °C, pH_{opt} = 2.5) demonstrated that this enzyme has some unusual properties, namely, concerning the dynamics of the binuclear site (*6*−*7*), and the role of its electron donor in catalysis (*8*) and in proton translocation (*9*). One striking feature of this oxidase is that it lacks most of the residues of the K and D pathways, including the so-called essential Glu 278 (*Paracoccus denitrificans* oxidase numbering), being thus significantly divergent from the most studied ones (see refs *5* and *10* for review). However, more recently, the full pumping capability of the *A. ambivalens* was demonstrated, showing that the strict conservation of the D and K proton pathways is not necessary to have pumping of 1 H^+/electron (*11*).

Fourier-transform infrared (FTIR)[1] difference spectroscopy is a highly sensitive method to detect even subtle structural changes as well as protonation changes that accompany redox reactions of an enzyme. In this work, we focused on the analysis of the signals observed in the prominent spectra range from 1790 to 1710 cm^{-1}, where exclusively the

† Financial support is gratefully acknowledged from the following institutions: Deutsche Forschungsgemeinschaft SFB 472 (to P.H.), Fundação Calouste Gulbenkian (Programa Estímulo à Investigação, to C.M.G.), and Fundação para a Ciência e Tecnologia (POCTI/BME/36560/99, to M.T.).

* To whom correspondence should be addressed: Petra Hellwig, Institut für Biophysik, Universität Frankfurt, Theodor-Stern-Kai 7 Haus 75, 60590 Frankfurt, Germany. E-mail: hellwig@biophysik.uni-frankfurt.de. Tel.: ++49−69−6301−4227. Fax: ++49−69−6301−5838.

‡ Universität Frankfurt.

§ Departamento de Química, Universidade Nova de Lisboa.

Instituto de Tecnologia Química e Biológica, Universidade Nova de Lisboa.

[1] Abbreviations: FTIR: Fourier transform infrared, SHE': standard hydrogen electrode, UQ: ubiquinone; CQ: caldariella quinone.

10.1021/bi0205348 CCC: $25.00
Published on Web 04/30/2003

contributions from protonated aspartic and glutamic acid side chains are expected for proteins.

MATERIALS AND METHODS

Sample Preparation. The aa_3 oxidase from *A. ambivalens* was prepared as previously described in ref *11*. For electrochemistry studies, the sample was solubilized in *n*-decyl-β-D-maltopyranoside, 100 mM phosphate buffer (pH 6.5) containing 100 mM KCl and concentrated to approximately 0.5 mM using Microcon ultrafiltration cells (Millipore). Exchange of H_2O against D_2O was performed by repeatedly concentrating the enzyme and rediluting it in a D_2O buffer. H/D exchange was found better than 75% as judged from the shift of the amide II mode at 1550 cm^{-1} in the FTIR absorbance spectra (data not shown). Ubiquinone-2 (UQ-2) and caldariella quinone (CQ) solutions were obtained by dispersing the quinone in the same buffer. These solutions were each added in an equimolar amount to the protein sample. CQ was purified from *A. ambivalens* cells using the procedure described in ref *12*.

Electrochemistry. The ultrathin layer spectroelectrochemical cell for the UV/VIS and IR was used as reported previously (*13*). Sufficient transmission in the 1800 to 1000 cm^{-1} range, even in the region of strong water absorbance around 1645 cm^{-1}, was achieved with the cell path length set to 6−8 μm. The gold grid working electrode was chemically modified by a 2 mM cysteamine and a 2 mM mercaptopropionic acid solution mixed in a 1:1 ratio. To accelerate the redox reaction, 15 different mediators were added as reported in ref *14* (except $K_4[Fe(CN)_6]$) to a total concentration of 40 μM each. At this concentration, and with the path length below 10 μm, no spectral contributions from the mediators in the VIS and IR range could be detected in control experiments with samples lacking the protein, except for the PO modes of the phosphate buffer between 1200 and 1000 cm^{-1}. As a supporting electrolyte, 100 mM KCl was added. Approximately 5−6 μL of the protein solution was sufficient to fill the spectroelectrochemical cell. Potentials quoted with the data refer to the Ag/AgCl/3M KCl reference electrode; add +208 mV for SHE' (pH 7) potentials. All measurements have been performed at 5 °C.

FTIR Difference Spectroscopy. FTIR difference spectra as a function of the applied potential were obtained simultaneously from the same sample with a setup combining an IR beam from the interferometer (modified IFS 25, Bruker, Germany) for the 4000−1000 cm^{-1} range and a dispersive spectrometer for the 400−900 nm range as reported previously (*13*, *15*). In all experiments, the protein solution was first equilibrated at the initial potential of the electrode, and single-beam spectra in the IR range were recorded. Then, a potential step toward the final potential was applied, and the single beam spectrum of this state was again recorded after equilibration. Subsequently, difference spectra, as presented in this work, were calculated from the two single-beam spectra with the initial single-beam spectrum taken as the reference. No smoothing or deconvolution procedures were applied. The equilibration at the applied potential generally took less than 5−6 min in the potential range from −0.5 to 0.5 V. Equilibration times were determined by monitoring UV/Vis difference spectra on the same sample (data not shown), and the full reaction in the FTIR spectroscopy was monitored by double difference spectra until no changes were detected. Typically, 128 interferograms at 4 cm^{-1} resolution were co-added for each single-beam IR spectrum and Fourier transformed using triangular apodization. A total of 5−10 difference spectra were usually averaged. The noise level in the difference spectra was estimated to be around 25−50 × 10^{-6} absorbance units in the spectral range under consideration, except for the region of the strongly absorbing water bending and protein amide I modes at ca. 1650 cm^{-1} where the noise was slightly higher.

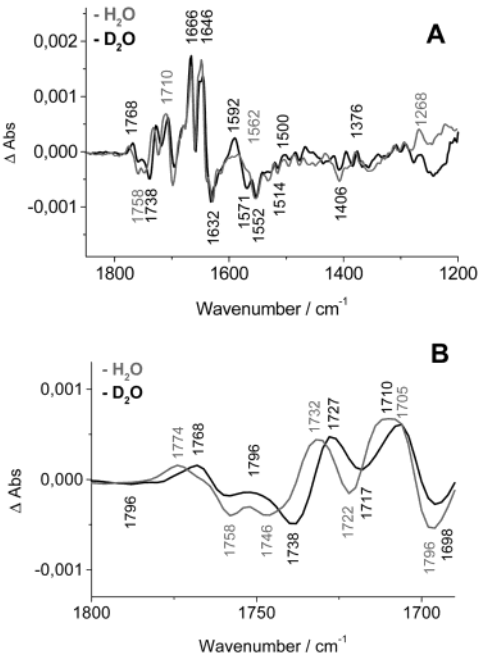

FIGURE 1: Oxidized-minus-reduced FTIR difference spectra of the aa_3 quinol oxidase from *A. ambivalens*. (A) Spectra for a potential step from −0.5 to 0.5 V vs Ag/AgCl equilibrated in H_2O (gray line) and D_2O (black line) buffer. For experimental conditions see Materials and Methods. (B) Enlarged view for the spectral range from 1800 to 1690 cm^{-1}, depicting the contributions of the protonated aspartic and glutamic acid side chains.

RESULTS

Electrochemically Induced FTIR Difference Spectra in H_2O and D_2O. Figure 1 A shows the oxidized-minus-reduced FT-IR difference spectra of the aa_3 oxidase from *A. ambivalens* for a potential step from −0.5 to 0.5 V, equilibrated in H_2O (gray line) and D_2O buffer (black line). Numerous distinct sharp bands appear throughout the spectrum, with half-widths typically below 5−10 cm^{-1}. The entirety of difference signals represents the total of molecular changes concomitant with the redox reactions. In the electrochemically induced FT-IR difference spectra, contributions from the porphyrin ring, the heme propionates, the vinyl substituent and contributions from the formyl groups can be expected from heme *a* and a_3. Besides the signals of the hemes, the reorganization of the polypeptide backbone and amino acid side chains occurring upon electron transfer of the redox active centers heme a/a_3, and Cu_B and coupled processes such as proton transfer can be expected to manifest in the spectra. The current purification procedure yields CQ-free oxidase (*16*).

Briefly, in the amide I range (1690−1620 cm^{-1}), difference signals at 1686, 1678, 1666, 1646, and 1620 cm^{-1}

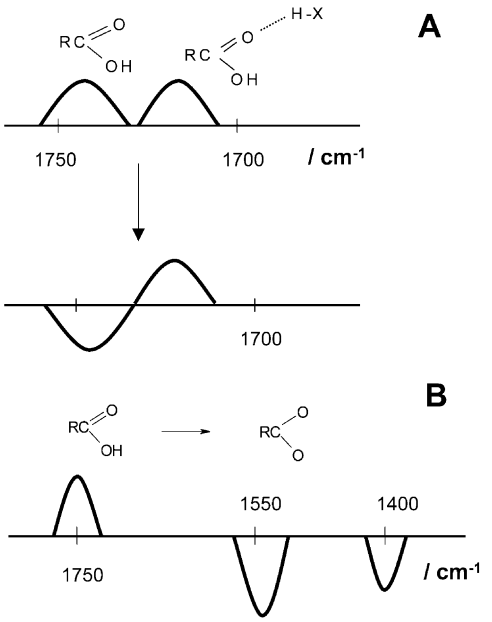

FIGURE 2: Schematic view of signals expected of an environmental change in the vicinity of a protonated acidic group (A) and a deprotonation reaction (B).

indicate absorbance changes of C═O modes caused by small alterations in the polypeptide backbone accompanying the redox process, as well as possible contributions from C═O modes of individual amino acid side chains (Asn and Gln). In the amide II range (1570−1520 cm^{-1}), coupled CN stretching and NH bending modes are expected. In addition, vibrational modes from aromatic amino acids and heme C═C modes from the porphyrin ring, for example at 1564, 1552, and 1530 cm^{-1}, are observable. Antisymmetric COO^- modes from deprotonated heme propionates and Asp or Glu side chains, caused by protonation/deprotonation of COOH groups, may also contribute in this spectroscopic range. Above 1680 cm^{-1}, signals from protonated heme propionates, and, above 1710 cm^{-1}, signals from protonated Asp and Glu are likely.

A particular problem of the assignment in the difference spectra is the superposition of signals from different constituents of the oxidase, which can lead to the possibility of multicomponent bands and may present ambiguities in the assignment. For example, the amide I range, is a spectral region particularly susceptible for overlapping bands, while, in contrast, the spectral range above 1710 cm^{-1} can be attributed very clearly to the contribution of the ν(C═O) mode from protonated aspartic and glutamic acids, the exact absorption depending on the hydrogen bonding.

Identification of the ν(C═O) Mode of COOH Groups. In the oxidized-minus-reduced FTIR difference spectra (Figure 1A) and in the enlarged view from 1800 to 1710 cm^{-1} (Figure 1B) positive modes are present at 1774, 1732, and 1710 cm^{-1} concomitant with the oxidation, and negative modes concomitant with the reduction are observable at 1796, 1758, 1746, and 1722 cm^{-1}. Upon H/D exchange (see black lines in Figure 1), a shift of 2−6 cm^{-1} is observed for the signals. These shifts of 4−10 cm^{-1} are characteristic for bands originating from protonated aspartates and glutamates as previously reported for other systems (*17*, *18*) and clearly indicate the presence of several protonated aspartic or glutamic acid side chains in the oxidized and reduced states

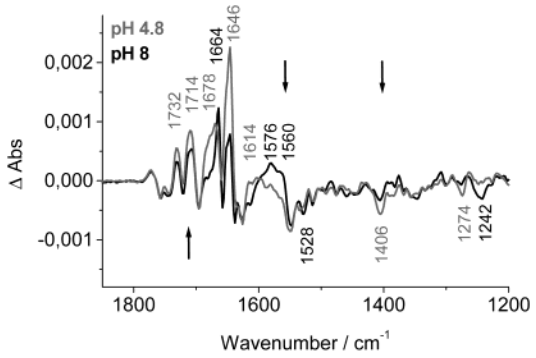

FIGURE 3: Oxidized-minus-reduced FTIR difference spectra of the aa_3 quinol oxidase from *A. ambivalens* for a potential step from −0.5 to 0.5 V vs Ag/AgCl equilibrated in a buffer at pH 4.8 (gray line) and 8 (black line) (A) and a double difference spectrum obtained by interactive subtraction of these lines (B).

of the enzyme, each located in different environments. The modes at approximately 1720−1710 cm^{-1} originate from residues coordinated by strong hydrogen bonds. The signals above 1758 cm^{-1} are observed at an unusually high wavelength. The position of these signals suggests a weak hydrogen bonding of the COOH group, such as would be found for an acidic residue buried in a hydrophobic region of the protein. The feature observed at 1774 cm^{-1} is the signal with the highest frequency so far observed for a ν(C═O) mode of a protonated acidic residue in any protein.

The acidic side chains discussed here, obviously rearranging due to the redox reaction, may be functional in the proton pathways of the enzyme. Two possible scenarios are possible to explain the observed spectral features: (i) the variation of the protein site surrounding the C═O group, i.e., the hydrogen bonding strength change upon the redox reaction, leading to an energy shift; (ii) the protonation/deprotonation of an acidic group, which causes the increase/decrease of the typical mode between 1790 and 1710 cm^{-1}. The expected shifts are described in Figure 2. The spectral features observed in Figure 1 could thus reflect both the protonation change of an acidic residue or the environmental change upon redox reaction. Especially in the second case, an increase of the pH should lead to a stronger deprotonation and to a decrease of the signals.

We note that it can be excluded that signals observed here may originate from changes in the protonation state of any Asp/Glu in the protein pointing toward the carboxylates near the surface. Indeed, any residue that is addressed by the redox reaction will contribute in the redox-induced FTIR difference spectrum. An overall protonation state change on the surface, however, does not occur in proteins as result of the reduction of the cofactors, since the reduction of a cofactor is most likely compensated in its direct environment. Otherwise, to our view, a well-defined protonation processes coupled to redox reactions would not be possible, as found for energy transducing proteins of the respiratory chain. In addition, we note that carboxylates at the surface, where the C═O group experiences more steric freedom, will contribute with a very broad mode around 1720 cm^{-1}.

Analysis of the pH Dependency of the Signals for the Acidic Groups. Figure 3 shows the oxidized-minus-reduced FTIR difference spectra obtained for samples equilibrated at pH 4.8 (gray line) and 9 (black line). We note at this point that despite *A. ambivalens* is an acidophile organism, the

intracellular pH of these organisms is fairly neutral and that thus the use of pH 6.5 is quite close to physiological conditions. Data at pH 3 was obtained, but not included, since no significant change of the protonated Asp/Glu side chains was observed between pH 3 and 5. In the spectral region from 1790 to 1710 cm^{-1}, a small increase of modes at 1732 and 1714 cm^{-1} can be seen at more acidic pH indicating a higher population of protonated residues from the aspartic and glutamic acid side chains involved here. Signals higher than 1740 cm^{-1} seem to be rather invariable pointing to the high pK_A value >8 of the residues involved here. Also at 1678 cm^{-1}, where the modes for the protonated heme propionates are expected, an increase of signal intensity can be described.

At lower frequencies, where the modes for the deprotonated acidic residues may be involved, the corresponding decrease of signals is seen. In detail, a signal between 1600 and 1560 cm^{-1} and at approximately 1406 cm^{-1} can be tentatively attributed to the $\delta(COO^-)^{as}$ and $\delta(COO^-)^{s}$ mode, respectively, reflecting a deprotonation reaction upon increase of pH (Cf. Figure 3). In the amide I region, at 1664, 1650, and 1646 cm^{-1}, a significant variation in signal intensity takes place upon pH change, indicating a structural change in the enzyme.

Involvement of Acidic Groups in Quinone Binding. The signals observed for the protonated aspartic or glutamic acid side chains may originate from residues involved in proton pumping or proton delivery to the oxygen reducing site but also from groups working as proton acceptors to the first electron donor, the quinol. Interestingly, a model of the enzyme indicated the presence of two glutamates in the putative proton pathways of the enzyme (*11*, *16*), and we hypothesize that these residues could be involved in the spectra observed here (see Figure 6 and discussion below). To probe for acidic residues possibly interacting with the quinone, the electron donor to the oxidase, spectra in its presence and absence have been compared. The native quinone from *A. ambivalens* is the caldariella quinone. The purified enzyme used in the present studies lacks any detectable amount of residual quinone. Since the *aa*$_3$ oxidase from *A. ambivalens* is additionally capable to react with ubiquinone, the effect of ubiquinone binding was also studied.

Figure 4 shows the effect of the addition of UQ-2 (A) or CQ (B) on the signals of the protonated aspartic and glutamic acid side chains. Clearly, a variation in intensity takes place for the signals between 1750 and 1720 cm^{-1} indicating an interaction. There are essentially two possible types of interaction taking place here: First, an hydrogen bonding of the added quinone with one or two protonated acidic side chains is likely, thus changing the C═O bonding. This hydrogen bonding could change the peak position or the intensity of the C═O group, the mode being directly coupled to the interacting -OH group. As an additional explanation for the signal variation, a shift of a protonated aspartic or glutamic acid could be the indirect consequence of the accommodation of the quinone at the protein site. Since no significant decrease of a signal is observable, a protonation change can be excluded to be coupled with the binding. The structurally distinct quinones UQ-2 and CQ do not necessarily interact with the protein at the same location, but a relatedness of the sites is expected to allow for similar electron transfer.

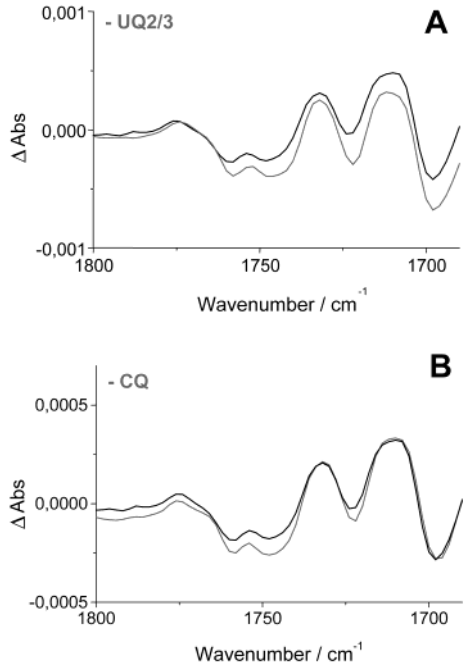

FIGURE 4: Oxidized-minus-reduced FTIR difference spectra for a potential step from −0.5 to 0.5 V vs Ag/AgCl measured in the presence of UQ-2 (A) and CQ (B) (gray line) in direct comparison to the sample devoid of quinone (black line). For experimental conditions, see Materials and Methods.

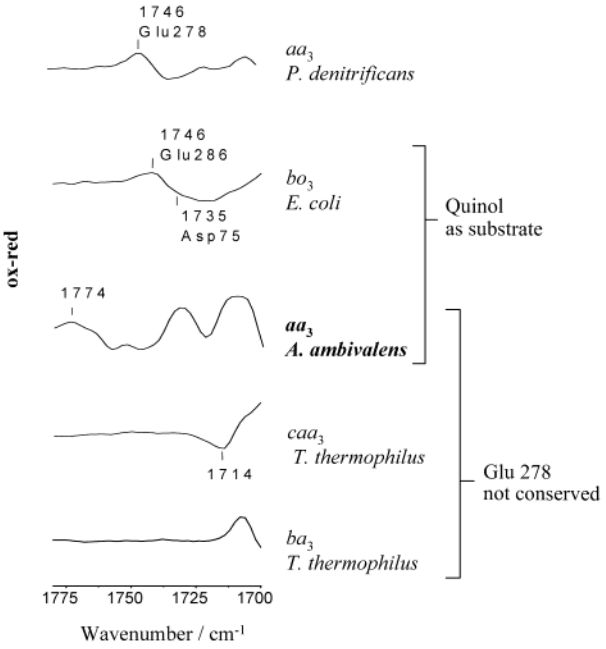

FIGURE 5: Comparison of the spectral range from 1800 to 1690 cm^{-1} for prominent members of the heme-copper oxidase superfamily. (See refs *14* and *21*−*23*).

DISCUSSION

The *aa*$_3$ oxidase from *A. ambivalens* represents a divergent member of the heme copper oxidase family. A significant number of amino acids, previously suggested to be canonical residues for proton conduction in this enzyme family, are not conserved. In this study, we used electrochemically induced FTIR difference spectroscopy to identify residues involved in redox coupled protonation changes. Figure 5 displays a comparison of the spectral region from 1780 to

1700 cm^{-1} as seen for oxidized-minus-reduced FTIR difference spectra for prominent members of the oxidase family. For the cytochrome *c* oxidase from *P. denitrificans* difference modes at 1746/1734 cm^{-1} have been observed and attributed to Glu278 (*14*). In the quinol oxidase from *Escherichia coli* similar changes were also assigned to the equivalent residue (*19*, *20*), in addition to the identification of a protonation partner of the quinone, Asp75 (*21*). In the *Thermus thermophilus* cytochrome *c* oxidases, where Glu278 is also not conserved, a complete absence of any signal from protonated aspartic or glutamic acids was observed (*22*, *23*). The absence of those signals for these enzymes shows clearly that unspecific rearrangements can be excluded.

This direct comparison of features in the spectral range from 1790 to 1710 cm^{-1} shows how unusual the significant number of signals is among heme-copper oxidases (Figure 5). On the basis of the experiments at different pH values, the modes at 1732 and 1714 cm^{-1} are likely to reflect protonation reactions within the enzyme. The position of these signals suggests residues located in hydrophilic regions of the protein. The modes higher than 1750 cm^{-1} seem rather invariant to the pH change and reflect modifications of the environment, i.e., of a weak hydrogen bonding, associated with the redox reaction. Overall, a minimum of four protonated aspartic or glutamic acid side chains are participating in the observed process, but a higher number of residues may be involved. These modes may originate either from residues involved in proton pumping or proton delivery to the oxygen reducing site, or from groups working as proton acceptors/donors to the first electron acceptor, the quinone. The high pK_a value of some of these residues, as identified from only small changes upon pH change, indicate that these residues may be involved in proton conduction without changing their bulk protonation state: only a small fraction of protonation/deprotonation may be sufficient for a residue to be involved, transiently, in a proton path. In addition, the environment of one or more residues may change during the catalytic cycle, due either to local protein conformational changes (including rearrangements of hydrogen bonds networks) or to long-range electrostatic effects, thus enabling the residue to uptake/release a proton.

Analysis of a structural model of the *A. ambivalens* enzyme shows the presence of two glutamates in a putative proton pathway: Glu80 and Glu83, both located in helix II. Figure 6 depicts the location of these residues, as well as a few other selected glutamates and aspartates that are located closely to the redox centers. Considering that the signals above 1758 cm^{-1} may be attributable to acidic residues in an hydrophobic environment, the Glu80, 83 but also Asp74 could be involved in the observed spectra. Noteworthy, these residues are not conserved in other oxidases, thus reinforcing the hypothesis that the observed features could be assigned to any of them. Quite importantly, *A. ambivalens* Glu 80 was proposed to be part of a proton channel (*11*), which was corroborated by a double mutant of the *Rhodobacter sphaeroides* aa_3 oxidase, which mimics the *A. ambivalens* enzyme, i.e., in which Glu286 was substituted by an Ala and Ile122 from helix II was substituted by a glutamate, equivalent to the *A. ambivalens* Glu80: this mutant retains its capability of full proton pumping (*24*).

Recently, the quinone binding site for the cytochrome bo_3 quinol oxidase from *E. coli* was identified close to the low spin heme (*25*, *26*). Interestingly, Glu47, also depicted in the structural model in Figure 6, seems to be located in the same region of the protein.

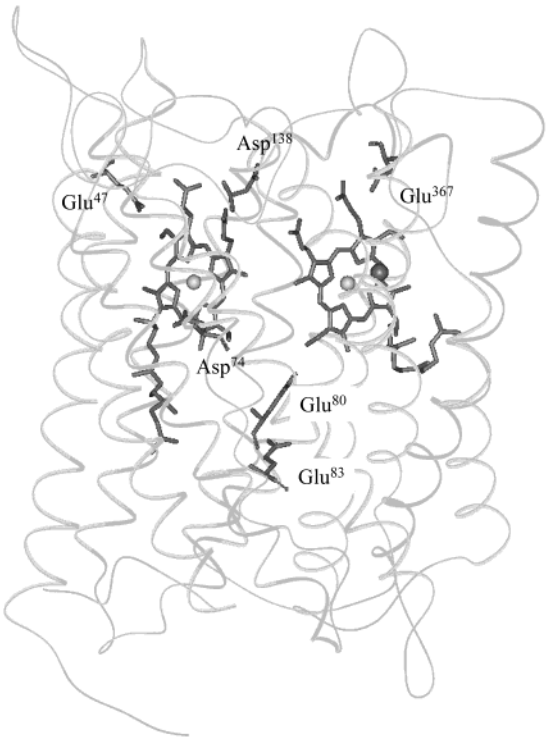

FIGURE 6: Structural model of the *A. ambivalens* aa_3 quinol oxidase highlighting six selected protonatable residues in the vicinity of the redox centers. The model was kindly provided by Drs. A. Kannt and H. Michel (MPI für Biophysik, Frankfurt, Germany).

ACKNOWLEDGMENT

A. Kannt and H. Michel (MPI für Biophysik, Frankfurt, Germany) are acknowledged for the structural model of the *A. ambivalens* oxidase. We thank W. Mäntele (Institut für Biophysik, Universität Frankfurt) for his continuous support.

REFERENCES

1. Ferguson-Miller, S., and Babcock, G. T. (1996) *Chem. Rev. 96*, 2889−2907.
2. Michel, H., Behr. J., Harrenga, A., and Kannt, A. (1998) *Annu. Rev. Biophys. Biomol. Struct. 27*, 329−356.
3. Mogi, T., Tsubaki, M., Hori, H., Miyoshi, H., Nakamura, H., and Anraku, Y. (1998) *J. Biochem. Mol. Biol., Biophys. 2*, 79−110.
4. Garcia-Horsman, J. A., Barquera, B., Rumbley, J., Ma, J., and Gennis, R. B. (1994) *J. Bacteriol. 176*, 5587−5600.
5. Pereira MM, Santana M., and Teixeira M. (2001) *Biochim. Biophys. Acta 1505*, 185−208.
6. Aagaard, A., Gilderson, G., Gomes, C. M., Teixeira, M., and Brzezinski, P. (1999) *Biochemistry 38*, 10032−41.
7. Aagaard, A., Gilderson, G., Gomes, C. M., Ädelroth, P., Teixeira, M., and Brzezinski, P. (2000) *Biochim. Biophys. Acta Bioenerg. 1503*, 261−270.
8. Giuffrè, A., Gomes, C. M., Antonini, G., D'Itri, E., Teixeira, M., and Brunori, M. (1997) *Eur. J. Biochem. 250*, 383−388
9. Das, T. K., Gomes, C. M., Teixeira, M., and Rousseau, D. L. (1999) *Proc. Natl. Acad. Sci. U.S.A. 96*, 9591−6.
10. Pereira, M., Gomes, C. M., and Teixeira, M. (2002) *FEBS Lett. 522*, 14−8.
11. Gomes, C. M., Backgren, C., Teixeira, M., Puustinen, A., Verkhovskaya, M. L., Wikström, M., and Verkhovsky, M. I. (2001) *FEBS Lett. 497*, 159−64.

12. De Rosa, M., De Rose. S., Gambacorta, A., and Minale, L. (1977) *J. Chem. Soc., Perkin Trans. 1*, 653−657.
13. Moss, D., Nabedryk, E., Breton, J., and Mäntele, W. (1990) *Eur. J. Biochem. 187*, 565−572.
14. Hellwig, P., Behr, J., Ostermeier, C., Richter, O.-M. H., Pfitzner, U., Odenwald, A., Ludwig, B., Michel, H., and Mäntele, W. (1998) *Biochemistry 37*, 7390−7399.
15. Mäntele, W. (1993) *Trends Biochem. Sci. 18*, 197−202.
16. Gomes, C. M. (1999) Oxygen utilisation by prokaryotes − Redox proteins from Archaea and anaerobic Bacteria. Ph.D. dissertation, Instituto de Tecnologia Química e Biológica, Universidade Nova de Lisboa, Oeiras.
17. Siebert, F., Mäntele, W., and Kreutz, W. (1982) *FEBS Lett. 141*, 82−87.
18. Pinchas, S., and Laulicht, I. (1977) *Infrared Spectra of Labelled Compound*, Academic Press, London, New York.
19. Lübben, M., Prutsch, A., Mamat, B., and Gerwert, K. (1999) *Biochemistry 38*, 2048−2056.
20. Yamazaki, Y., Kandori, H., and Mogi, T. (1999) *J. Biochem. 126*, 194−199.
21. Hellwig, P., Barquera B., Gennis, R. B. (2001) *Biochemistry 40*, 1077−82.
22. Hellwig, P., Soulimane, T. Buse G., and Mäntele, W., (1999) *Biochemistry* 38, 9648−9658.
23. Hellwig, P., Soulimane, T., and Mäntele, W., (2002) *Eur. J. Biochem. 269*, 4830−8.
24. Aagaard A., Gilderson, G., Mills, D. A., Ferguson-Miller, S., and Brzezinski, P. (2000) *Biochemistry 39*, 15847−50.
25. Abramson, J., Riistama, S., Larsson, G., Jasaitis, A., Svensson-Ek, M., Laakkonen, L., Puustinen, A., Iwata, S., and Wikström, M. (2000) *Nat. Struct. Biol. 7*(10) 910−917.
26. Hellwig, P., Yano, T., Ohnishi, T., and Gennis, R. B. (2002) *Biochemistry 41*, 10675−9.

BI0205348